Cellular Physiology and Biochemistry

Cell Physiol Biochem 2026;60:175-188
DOI: 10.33594/000000859
Published online: 10 April 2026
Accepted: 4 April 2026

Original Paper

Tumor Destructive Mechanical Impulse (TMI) Treatment of Solid Tumors. Part III: Transcranial Application, Immune Profile, Blood-Brain Barrier, Neuroprotection, Neuromodulation and Neurostimulation

Axel Erich Theuer[a] Stella Exner[b] Ioannis Thomas[c,d] Florian Lang[e] John David Mullins[f] John Warlick[g] Gerd Strassmann†[h] Thomas K. Eigentler[a] Gerhard Franz Walter[i]

[a]Department of Dermatology, Venerology and Allergology, Charité University Hospital, Berlin, Germany, [b]Pediatrician's Office, Marktoberdorf, Germany, [c]Department of Dermatology, University of Tübingen, Germany, [d]EDOEAP (Unified Journalistic Organization of Supplementary Insurance and Health), Athens, Greece, [e]Institute of Immunology, University of Duisburg-Essen, Essen, Germany, [f]Shepherd Center Wound Clinic, Piedmont Atlanta Hospital, Atlanta, GA, USA, [g]SoftWave Tissue Regeneration Technology, Alpharetta, GA, USA, [h]Department of Radiotherapy and Radiation Oncology, University of Marburg, Germany, [i]International Neuroscience Institute, Hannover, Germany

Key Words
Tmi treatment of tumors • Transcranial application • Primary and secondary brain tumors • Neuro-regenerative effects

Abstract
Background/Aims: We explored the fundamental feasibility, technical frame conditions and effectiveness of transcranial Tumor Destructive Mechanical Impulse (TMI) treatment of brain tumors. ***Methods:*** The optimal treatment parameters (total energy required, energy flux density, shock wave frequency) and applicator positions were explored and defined with respect to the special conditions given by propagation of shock waves through the skull. ***Results:*** As first clinical observations, **w**e present the outcome of transcranial TMI treatment in two cases with brain metastases of malignant melanoma. In both cases, regression of metastases as well in the brain as in other sites was observed, in one of the cases with a complete tumor free recovery. ***Conclusion:*** In these cases, there were no identifiable signs of impairment of the surrounding brain tissue, and even indications of neuro-regenerative effects as described in the cited experimental literature, so that transcranial TMI treatment of brain tumors may be applied for further systematic investigation without any currently discernible risk for the intact surrounding brain tissue.

Prof. Dr.-Ing. habil. A. Erich Theuer
Department of Dermatology, Venerology and Allergology, Charité University Hospital, Berlin, Germany
Phone: +49-162-3884554, Email: prof.theuer@gmail.com

Introduction

Because of the concerns about the potential damage to the human brain or spinal cord by shock waves, no clinical studies were carried out to explore the clinical use of shock waves in the treatment of human central nervous system tumors.

Tumor Destructive Mechanical Impulse (TMI) shock wave treatment exploits rapid pressure fluctuations, including both compression and tensile phases, to initiate cavitation bubbles, shear forces, and localized micro-lesions inside tumors. The collapse of cavitation bubbles generates extremely high local stresses capable of affecting cell membranes, organelles, and extracellular matrix components. TMI treatment with pressure and strains on tumor cells may induce an immunological abscopal effect attacking the primary tumor as well as its metastases without disadvantageous side effects.

Basic technical parameters and applicator design for tumor destructive mechanical impulse (TMI) treatment of patients suffering from malignant tumors have been patented [1-4]. The biological preconditions including biomechanics and physiological effects as well as computational simulation for safe technical generator and applicator design have been established, thereby, paving the way for preclinical application in animal experiments and clinical applications of TMI treatment, both leading to an immunological abscopal effect [5-6].

Regarding transcranial applications, focused ultrasound has been experimentally and clinically applied for the treatment of brain tumors [7-8]. Further, Tumor Treating Fields (TTFs) as therapy for glioblastoma multiforme are alternating electric fields of low-intensity and intermediate-frequency (100-300 kHz) that exert physical forces interfering with cell organelles [9]. However, the physico-mechanical difference between ultrasound waves and electric TTFs in comparison to shock waves as in TMI treatment has consequences for the respective therapeutic applicability.

We present two cases with transcranial TMI treatment for tumors, amongst them an exceptional case in a unique, non-reproducible situation in more detail. This paradigmatic patient suffered from three different malignant tumors for 19 years. Two and a half years before his death the palliative patient received TMI treatment, and ten months before his death transcranial TMI treatment was applied as a last resort in a quite hopeless situation. The transcranial TMI treatment resulted in astonishing improvements in the clinical situation, with an unexpected life extension by almost one year in comparatively good life-quality, before the patient finally died from his complex illness. The second case of brain metastases from malignant melanoma fully recovered after transcranial TMI treatment and is tumor-free.

Materials and Methods

TMI generator technologies (brief)

TMI refers to the therapeutic delivery of short, high-amplitude acoustic impulses to tissues. TMI generators include electrohydraulic, electromagnetic, and piezoelectric systems; all deliver steep pressure fronts with a tensile tail that can induce intracellular cavitation within the tumor cells (Table 1).

The principles of transcranial generator and applicator design have already been described [TMI part II]. Energy losses at impedance mismatches and wavefront scattering necessitate careful trajectory selection and soft-focus strategies that cover the lesion with adequate safety margins.

Biophysical considerations and transcranial targeting

Transcranial TMI impulses generated extracorporeally must traverse soft tissue, cortical bone (zona compacta) with high acoustic impedance and attenuation, and permeate trabecular networks (zona spongiosa) and again the inner zona compacta to reach the cerebral target (Table 2).

These different biophysical properties of the tissue layers to be traversed by transcranial TMI lead to different technical material properties for computational simulation. The detailed technical properties were determined from own measurements [6] and from the extensive relevant literature (Table 3).

Computational simulation

To ensure patient safety and reproducibility, patient-specific DICOM (Digital Imaging and Communications in Medicine) data were segmented using Simpleware ScanIP® (Synopsys Inc.) and subsequently imported into ANSYS SpaceClaim (ANSYS® SpaiceClaim; version 2024.R2, ANSYS Inc.) for geometry preparation enabling coupled device-tissue simulations under clinical pressure wave forms. The resulting anatomical models were subsequently simulated in ANSYS Explicit Dynamics (ANSYS® Mechanical/Fluent/CFX, version 2024.R2, ANSYS Inc.).

In parallel, DICOM data were processed using MATLAB®/TABLIN and converted into OnScale® (formerly PZFlex, OnScale Inc.), an explicit acoustic and time-domain solver designed for high-frequency

Table 1. Technical options for TMI generator technologies

Technology	Working Principle, Focal Properties, and Cavitation Behavior
Electrohydraulic (EH)	Spark-gap discharge in water creates a plasma bubble and a shock wave, focused by an ellipsoidal reflector; broad focal zone, strong cavitation propensity; historically used in lithotripsy and orthopedic
Electromagnetic (EM)	Lorentz-force membrane or coil-driven acoustic pulse launched into a lens or reflector. Reproducible output, intermediate focal volumes; cavitation controllable via energy and pulse profiling
Piezoelectric (PZ)	Phased piezo array elements on a spherical cap generate converging pulses. High spatial precision and small focus volumes; cavitation can be minimized or enhanced depending on drive settings

Table 2. Biophysical properties of the different tissue layers to be traversed by TMI

Tissue Layer	Biophysical Properties and Acoustic Behavior
Zona compacta	Highly mineralized dense outer bone layer Acoustic impedance mismatch with surrounding soft tissue High attenuation and reflection of pressure waves Significant wavefront distortion and energy loss at this interface
Zona spongiosa	Porous, vascularized inner bone matrix Better wave transmission due to reduced acoustic impedance Allows for scattering and partial focusing of the wavefront Offers pathways for energy diffusion toward the bone marrow
Bone marrow	Complex microenvironment between trabeculae and bone marrow

Table 3. Technical material properties of the different tissue layers to be traversed by TMI

Mechanical Property	Symbol	Zona compacta	Zona spongiosa	Bone marrow
Density	ρ	1800–2000 kg/m^3	100–1200 kg/m^3	1000–1060 kg/m^3
Young's modulus	E	17–20 GPa	50–2000 MPa	2–50 kPa
Poisson's ratio	ν	0.30	0.20–0.30	0.45–0.49
Shear modulus	G	6–7 GPa	—	—
Bulk modulus	K	13–15 GPa	—	2–2.2 GPa (fluid-like)
Compressive strength	—	130–200 MPa	2–12 MPa	—
Dynamic viscosity	μ	—	—	0.01–0.1 Pa·s

pressure wave propagation analysis in complex biological media, suitable to predict pressure fields, focal volumes, and attenuation through bone. The outputs of the numerical solution of the FEM propagation models include total energy, energy flux density, impulse count and frequency, and the optimal placement of the TMI-treatment applicator.

TMI treatment devices

For the delivery of shock waves, the piezoelectric PiezoWave^2 device (Elvation Medical GmbH) [10] and the electrohydraulic OrthoGold100® device (MTS Medical UG) [11] were used.

The PiezoWave^2 device with linearly focused shock waves enables, compared to conventional, point-focused shock waves, a more homogeneous and effective application and variability in shock wave modulation. It offers a choice between classically focused, linearly point-focused, and planar pressure waves.

For the OrthoGold100® device three applicators can be used differing primarily in the focusing of the shock wave focus field. With the dark blue applicator generated shock wave is highly focused. With the yellow applicator the shock waves are emitted less focused, the therapeutic focus field is therefore larger and deeper, achieving a penetration depth of up to 120 mm and a width of up to 25 mm. The light blue applicator represents a kind of hybrid between the dark blue and yellow applicators (Fig. 1).

The electrohydraulic applicator generates not only pressure pulses but also – as part of the capacitive discharges – light pulses which could act as photosensitive amplifiers. The entire therapeutic device arrangement requires minimal space (Fig. 2).

The applicator delivers the acoustic waves to the treatment target by achieving electrohydraulic contact via the water membrane and ultrasound gel. At the reflector, the acoustic wave is unfocused. Positioning of the reflector allows transmitting the acoustic wave onto the treatment target. The coupling of the applicator to the extracorporeal treatment area is to be carried out with a silicone membrane and ultrasound gel.

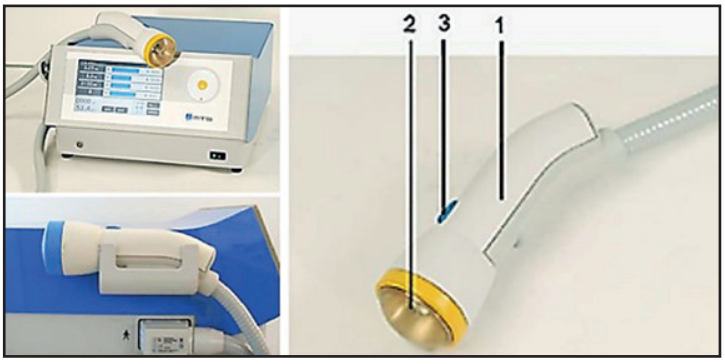

Fig. 1. The compact OrthoGold100® device with light blue and yellow applicators, 1 Applicator housing, 2 Water membrane 3 Acoustic wave release button.

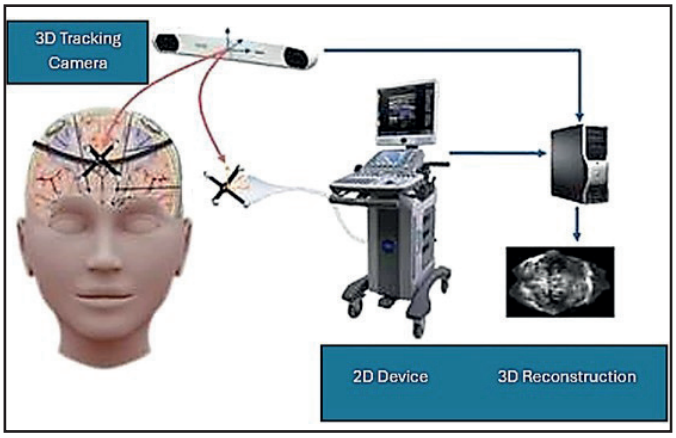

Fig. 2. Device arrangement for TMI treatment.

Case Reports

The presented cases are first exploratory clinical observations with inherent limitations of interpretation. Therefore, in Berlin, a randomized clinical trial of TMI-treatment of malignant melanoma, including brain metastases as in the cases presented, and, in Hannover, another randomized clinical trial of transcranial TMI-treatment of glioblastoma are in planning.

The experimental TMI treatment of patients was approved by the Ethics Committee at the Medical Faculty of the Eberhard Karls University and at the University Hospital of Tübingen (PNR150/2019BO2). All patients provided written informed consent to participate in an individual healing attempt, agreed – fully aware of the experimental character of transcranial attempts of TMI treatment – to repeated approaches as described below, and consented to the use of their de-identified clinical data for publication.

Case A

The 73 years old male patient was medical doctor himself. He provided written informed consent to participate in an individual healing attempt, agreed – fully aware of the experimental character of a first transcranial attempt of TMI treatment – to repeated approaches as described below, and consented to the use of his de-identified clinical data for publication. He has a long history of three malignant tumors, the first occurring in 2007:

2007

Superficial spreading malignant melanoma (Clark level III pT1a9), surgically resected.

2013

Prostate carcinoma (pT2c, pN0, R0, Gleason 7a), surgically resected, and surgical removal of regional lymph nodes.

2018

Diffuse large Non-Hodgkin B-cell lymphoma with strong proliferative activity (stage IIIA), chemotherapy, antibody therapy, CHOP regimen.

All three tumors were successfully treated following standard treatment regimens.

July 2023

After five years of being free of symptoms, a rapidly growing, parotid-adjacent tumor on the right side occurred leading to facial palsy. An attempt to surgically remove the tumor was aborted due to risk to the facial nerve. An F-18-FDG PET whole-body CT scan revealed several disseminated hepatic metastases, osseous metastases in the pelvis and in the 5th dorsolateral rib.

Histology of a biopsy from a hepatic metastasis as well as from a biopsy of the osteolytic region at the 5th rib, confirmed a recurrence of malignant melanoma. At this moment, the patient was in significantly reduced general condition with bad prognosis. The patient has been receiving oncological combination therapy with two immune checkpoint inhibitors, Ipilumab and Nivolumab. In parallel, an ultrasound-guided, once-weekly piezoelectric TMI treatment in the right parotid region was initiated. For this purpose, the PiezoWave^2 device was used with a gel pad (shallow penetration depth Gelpad Nos. 5 and 10). The frequency used was between 2 and 4 Hz per treatment, with 3 Hz being the most common frequency. Depending on pain sensitivity and tolerance, 1000-1500 impulses were applied per session with an energy flux density of 0.12 mJ/mm^2. Following four immune checkpoint combination therapy sessions and eleven treatments with piezoelectric TMI treatment, a distinct regression after two months and a complete remission of the parotid-adjacent tumor as well as complete concomitant remission of the facial palsy occurred within four months (Fig. 3).

Alongside the TMI treatment of the parotid region, TMI treatment of the pelvis metastasis using the PiezoWave^2 device was performed simultaneously, precisely localizing the metastatic area measured in the PET-CT scan and based on patient-specific FEM simulation analyses. The deepest penetration depth was achieved with Gelpad 60, at a frequency of 2 Hz. Each treatment delivered 3000 impulses with an energy flux density of 0.35 mJ/mm^2. In a CT scan six months later, a significant reduction in bone metastases was observed as well

as a complete remission of the hepatic metastases not directly treated with shock waves; however, a new pelvic metastasis had occurred. The metastasis at the 5th rib had disappeared (Fig. 4).

Though the patient was affected by both the oncological disease and the side effects of the drug therapy, to consolidate and continue the evident therapeutic efficacy, regular TMI treatment of the new metastasis in the pelvic region was resumed with the OrthoGold100® device. The patient was treated 14 times over a six-month period. Each treatment involved a combination of the focused technique with the dark blue applicator and the non-focused technique with the yellow applicator. The deepest penetration depth was selected, along with energy flux density of 0.18 mJ/mm^2 or 0.27 mJ/mm^2, applying 2000 impulses per applicator, thus a total of 4000 impulses per session. After TMI treatment, native CT scans showed a distinct regression of the new pelvic metastasis and unchanged sclerosis of the known bone metastases.

March 2025

After a period of complete pain and symptom relief, the patient experienced sudden and rapidly progressive paralysis of the left side of his body with a rapid loss of the ability to walk. Subsequently, significant deficits in spatial perception developed. Imaging of the skull revealed a suspected hemorrhagic metastasis in the region of the right precentral gyrus and another prominent metastasis in the region of the right thalamus. A neurosurgical decompression of the metastatic tumor in the right precentral gyrus was performed and provided histological confirmation of a metastasis of malignant melanoma. However, due to a rapid recurrence of paresis and an increase in the size of the thalamic metastasis, CyberKnife treatment of the affected area was performed. This also included the treatment of a newly developed right-sided cerebellar metastasis.

After exhausting all conventional methods and experiencing severe intolerance to oral medication with Trametinib and Dabrafenib, the patient was bedridden with left-sided

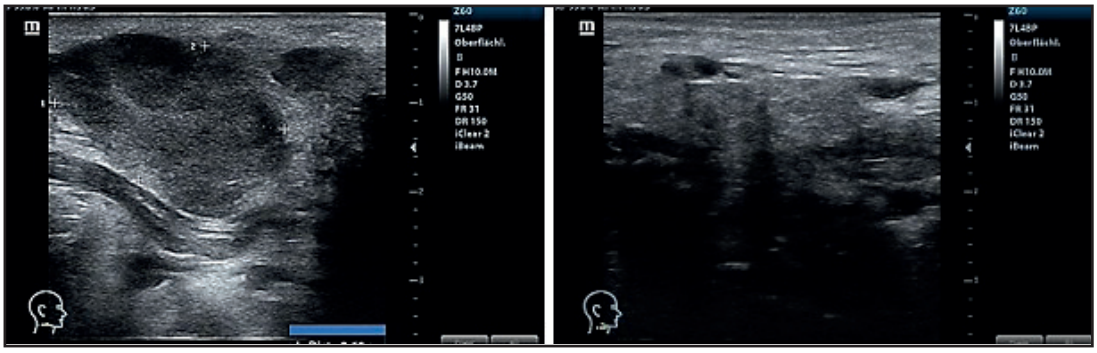

Fig. 3. Sonography of the parotid-adjacent tumor before TMI treatment (left) and regression two months later after TMI treatment (right).

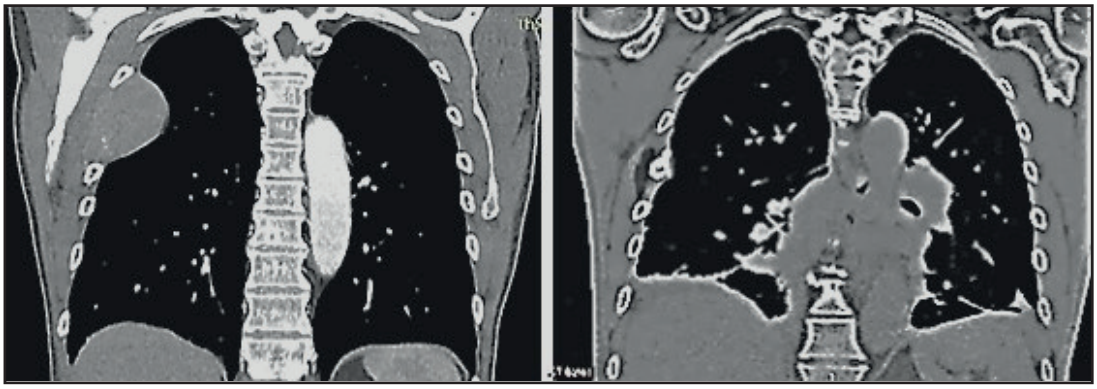

Fig. 4. Metastasis at the 5th rib before TMI treatment (left) and disappearance of the metastasis six months after TMI treatment (right).

paresis and severely impaired consciousness in a palliative situation. Further imaging showed a progression of the thalamic metastasis as well as several small right-sided cerebellar metastases. The patient was given up expecting his imminent death.

Therefore, transcranial TMI treatment has been administered as a last resort. Nine focused TMI treatments of the affected right thalamic area were performed twice weekly, using a combination of piezoelectric techniques with the PiezoWave^2 device (penetration depth 40-50 mm, energy flux density 0.1-0.15 mJ/mm2 adjusted for tolerance, frequency 3 Hz, applying 600-200 impulses per session adjusted for tolerance) and electrohydraulic techniques with the OrthoGold100® device (light blue applicator, energy flux density 0.09–0.12 mJ/mm^2, frequency 2-4 Hz, alternating, impulses 500-1200 per session, each adjusted for tolerance in case of the patient's limited general condition). Following completion of the focused transcranial TMI treatment of the thalamic region, the area of the right-sided cerebellar metastasis was treated seven times in the same way with a combination of piezoelectric and electrohydraulic techniques. Prior to the treatments, curcumin infusions (150 mg per dose), an active constituent of the ancient medicinal herb *Curcuma longa L.*, were administered twice weekly to support the immune system and to increase the efficiency of the electrohydraulic TMI treatment via a photosensitive effect. A total of 13 curcumin infusions were given.

From the outset, all combined piezoelectric and electrohydraulic treatments were subsequently expanded with a gentle, putative neuro-regenerative treatment of the entire brain using circular movements around the skull exclusively applying electrohydraulic technology with the OrthoGold100® device, always unfocused, with higher frequencies and significantly lower power outputs, and with a comparatively higher number of dual-state pulses (yellow applicator, energy flux density 0.02–0.05 mJ/mm^2, frequency 3 Hz, impulses 1500-3000 per session), adjusted for tolerance.

With temporary clinical improvement and increased patient tolerance, the established treatment of the pelvic bone metastasis using with the OrthoGold100® device was resumed (light blue applicator, energy flux density 0.23 mJ/mm^2, frequency 2 Hz, 2000 impulses per session). However, during the treatment, the patient became somnolent and had to be carefully supported at home with the assistance of the entire family. Apart from curcumin infusion therapy, life-sustaining fluid therapy, and TMI treatment, all other medications were discontinued, even the dexamethasone initially administered to reduce intracranial pressure.

August 2025

After transcranial TMI treatment as described, the patient was becoming increasingly alert and showed improvement in all neurological investigations. With the support of the physiotherapist, he could now walk short distances and climb one flight of stairs, use the toilet independently, his spatial awareness was steadily improving, he could eat independently, and had complete recollection of all events up to the onset of somnolence. He had no memory of the eight weeks of somnolent state. A follow-up MRI of the skull shows the previously identified hemorrhagic area surrounded by a glial capsule and a perifocal edema, but no further progression of the metastasis. The TMI reated thalamic metastasis had shrunk considerably though it is unsure if there remained still vital tumorous tissue (Fig. 5).

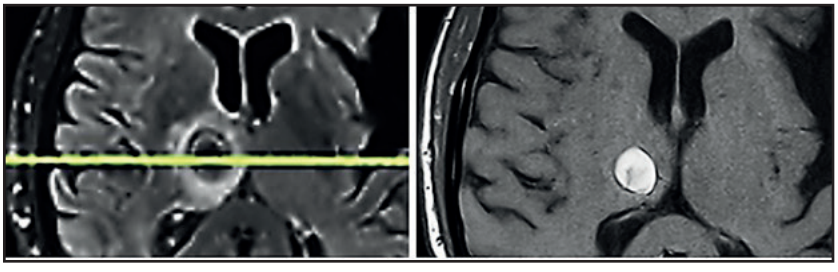

Fig. 5. Metastasis in the right thalamus before transcranial TMI treatment with pronounced perifocal edema (left) and five months after TMI treatment; notably the brain tissue is not impaired by the transcranial TMI treatment (right).

It must be underlined that the surrounding brain tissue was not impaired or damaged by TMI treatment, so that the patient clinically improved, unexpectedly gained again full neurological control, could leave the hospital and return home.

January 2026

While the patient remained in relatively good health, three weeks before his death, a quantitative immune profile (EDTA-blood) was analyzed (Table 4).

The present quantitative immune profile reveals an overall picture of systemic immune activation with a marked shift in the adaptive immune cell distribution, while the immune system's regenerative capacity remains intact. The leukocyte count is moderately elevated, suggesting a systemic inflammatory or immune-activated state, while the absolute lymphocyte count is within the normal range, indicating no global immunosuppression. However, a pronounced alteration of lymphocyte subpopulations is striking, with a significantly reduced total number of T cells, as well as decreased $CD4^+$ T helper cells and $CD8^+$ cytotoxic T cells. This pattern suggests less of a central production disorder and more of a functional redistribution or increased peripheral utilization of activated T cells, perhaps as part of an antigen-specific immune response with migration to tissues or tumor areas. This interpretation is supported by the preserved thymic reserve, indicating intact T-cell proliferation, and by the presence of activated T cells without evidence of a pronounced pre-activated or depleted T-cell population.

Particularly striking is the pronounced expansion of B cells with a significantly increased proportion of lymphocytes, indicating marked humoral immune activation, typically observed in the context of strong antigen exposure, immunological stimulation, or checkpoint-mediated immune responses. This pattern may be associated with an enhanced antibody response or increased antigen presentation. Concurrently, the CD8 T-cell population shows a shift towards differentiated effector and terminal effector cells, with reduced

Table 4. Quantitative immune profile (EDTA blood). Absolute values (/µl) and relative proportions (%) are given. Values outside the reference range are highlighted in red; values within the reference range are shown in green.

Parameter	Value (/µl)	Ref Min (/µl)	Ref Max (/µl)	Value (%)	Ref Min (%)	Ref Max (%)
General						
Immune Competence						
Immune Activation						
CD8+ T Cell Subpopulations						
Immune Tolerance						
Leukocytes	13200	4000	10000			
Lymphocytes	3472	1100	4000	26	20	44
T cells	684	900	2200	20	62	78
B cells	2638	74	324	76	7	19
NK cells	76	75	716	2	5	36
CD4+ T helper cells	344	590	1460	10	32	54
CD8+ T cells	295	300	930	8	23	40
Thymic reserve (CD31+)				55	43	
CD4/CD8 ratio	1,2	1	3			
Pre-activated T cells (CD25+)	7		78	0		6
Activated T cells (HLA-DR)	149		345	4		17
CD4+/CD8+ T cells				0,6		5
CD8+/CD28+ T cells	118	238	448	40	49	73
Naïve Tc cells	15	16	1000			
Central memory Tc cells	10	40	640			
Effector memory Tc cells	31	5	120			
Terminal effector Tc cells	113	25	280			
CD8+/CD28– T cells	177	100	370	60	26	51
Regulatory T cells (CD4+/CD25++/CD127low)	21	20	80	6,2	3	9
CD39+ Treg fraction				22		54
CD8/CD28 ratio	0,7	1	2,8			

numbers of naïve and central memory cells, suggesting antigen-driven differentiation and an active cytotoxic effector phase. The reduced CD8/CD28 ratio further supports the picture of chronic or persistent immune activation.

NK cells are at the lower end of the normal range or relatively reduced, which, in the context of adaptive immune activation, can be explained by functional recruitment or consumption. Overall, regulatory mechanisms do not appear dominant, as regulatory T cells are within the normal range and no pronounced immunosuppressive constellation is evident. Overall, there is no evidence of relevant systemic immunosuppression or pronounced tumor-induced immune tolerance.

February 2026

The patient died after he had an acceptable good quality of life until shortly before his death, surrounded by his family.

Case B

A now 76 years-old female patient suffered since 2013 from a metastatic malignant superficial spreading skin melanoma (pT3aN3cM1c) in the right gluteal area. After resection of the primary tumor and repetitive resections of cutaneous and subcutaneous metastases situated between the primary tumor and the regional lymph nodes (in-transit filiae), and metastases in the regional lymph nodes, and after immunotherapy cycles with Nivolumab, in 2020, an occipital brain metastasis occurred. Nivolumab immunotherapy was resumed, applying 25 cycles.

Five extracorporeal TMI treatments (4, 000 impulses each within 20 minutes) were applied to a cutaneous metastasis. As well the treated tumor as the not treated metastases regressed significantly.

In June 2024, transcranial TMI treatment of a new occipital metastasis was applied. The treated brain-metastasis regressed. Controls six, twelve and twenty months, the latter in February 2026, after transcranial TMI treatment did not show any new metastases and no vital tumor tissue in the glial scar remnants of the regressed metastasis (Fig. 6).

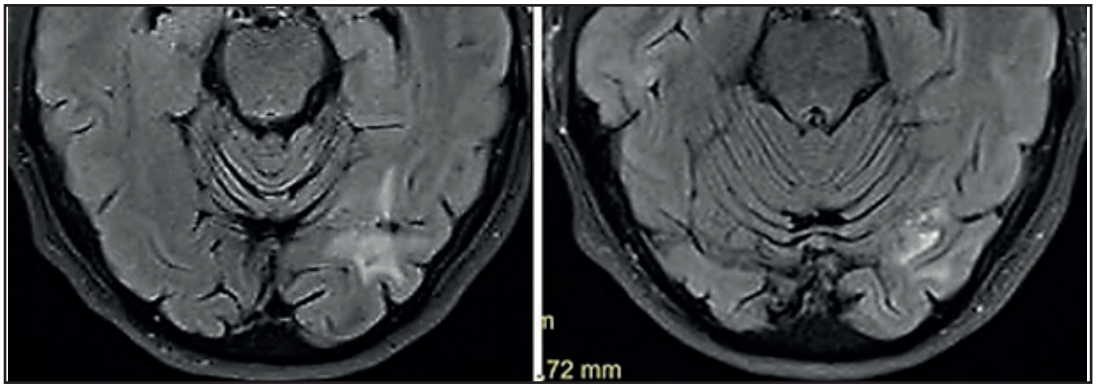

Fig. 6. Occipital metastasis six months (left) and twelve months (right) after transcranial TMI treatment with glial scar. Notably the brain tissue is not impaired by the transcranial TMI treatment

Discussion

The first case of this report describes the long-term course of a patient with multiple recurrences of metastatic malignant melanoma. The two additional malignomas, prostate carcinoma and diffuse large Non-Hodgkin B-cell lymphoma, suggest that a mutation of a suppressor gene, e.g. p53, might be present [12-13].

Alongside conventional oncological therapies, the addition of TMI shock wave treatment using piezoelectric and electrohydraulic methods resulted in the rapid regression of a parotid-adjacent metastasis and the remission of all hepatic metastases within a few months. Bone metastases also showed significant regression over the course of several years, accompanied by a visible clinical stabilization of the patient.

Immune profile

The immune profile shows a pattern of a biologically active, antigen-specific immune response with strong humoral activation, antigen-driven cytotoxic T-cell differentiation, and preserved immunological regenerative capacity. This is consistent with an active immune surveillance state and increased antigen exposure, as can be observed in the context of tumor antigen release, tissue destruction, or immunomodulatory therapies, without evidence of therapy-induced immune system exhaustion or relevant systemic immunosuppression. Thus, in the first case, an abscopal effect of TMI treatment has occurred as already described in other patients with malignant metastatic melanoma [5].

In the second case described, even a full tumor-free recovery of the patient could be achieved. For both patients, the reaction of the blood-brain barrier to transcranial TMI treatment may have played an important role.

Blood-brain barrier

The blood-brain barrier (BBB) remains a significant obstacle for immune cells to direct interact with brain tumor cells.

Acoustic energies such as ultrasound and shock waves are known to modulate tissue permeability and can be applied for repeated and transient BBB disruption [14-16]. Recently, it was found that shock waves modulate the blood-brain barrier in the rat brain without injection of contrast agents such as microbubbles [17]. Bubble-enhanced shock waves – avoiding shock wave overpressure, thus, within the parameters applied for TMI treatment – induce the transient opening of the BBB, providing access of immune cells to TMI treated brain tumors, but little is known about the molecular details of this process [18]. In animal experiments in rats (50 impulses, energy flux density 0.21 mJ/mm^2, frequency 5 Hz), the BBB opening could be precisely controlled in terms of depth, size and location [19].

There is one existing therapeutic approach, comparable with transcranial TMI treatment in so far that transcranial acoustic energy is used. In a clinical trial, the treatment of high-grade-glioma with microbubble-enhanced focused ultrasound showed that controlled BBB opening permitted localized drug delivery [20]; immunological effects as induced by retarded apoptosis we have experimentally seen after TMI treatment [6] are not reported.

In the present case A, one theoretical explanation could be the transfer of immunity via the permeable BBB to the cerebral target area. The immunity was previously acquired through several years of peripheral bone marrow TMI treatment, achieved through a comparatively small number of TMI shock wave sessions performed at a significantly low power. The role of the concurrently administered curcumin infusions remains unclear, as they could act as photosensitive amplifiers [21-22] in conjunction with the light effect of the electrohydraulic technique.

Neuroprotection

Shock waves have not previously been used as a treatment modality for brain tumors because of the lack of a suitable shock wave source and concerns about safety.

In military medicine, much attention has been given to effects of exposures to shock waves as a possible factor causing severe higher brain dysfunction and post-traumatic stress disorder, like symptoms in patients with mild to moderate blast-induced traumatic brain injury [23-24].

However, the parameters applied in TMI treatment are clearly "softer" than those originating from war-like circumstances. Toll-like receptors (TLRs) connect the innate immune system to the adaptive immune system. TLRs are present on the resident macrophages of the central nervous system and are also expressed by the neurons to allow them for production of proinflammatory agents such as interferons, cytokines, and chemokines [25]. It was shown that shock wave treatment via activation of the innate immune receptor TLR3 enhanced neuronal sprouting and improved neuronal survival in zebrafish and even in human spinal cord cultures [26]. TLR3 stimulation via TMI treatment could become a potent regenerative treatment option for lesions of the central nervous system.

Some experimental models are reported. The brains of Sprague-Dawley rats were exposed to shock wave generated with a holmium:yttrium-aluminum-garnet (Ho:YAG) laser, indicating possibilities for applying shock waves in various neurosurgical treatments such as cranioplasty, local drug delivery, embolysis, and pain management, with almost no damage to surrounding tissue in the rat brain [27].. After spinal cord injury, neural tissue repairment and regeneration is initiated by vascular endothelial shear stress which generates a frictional force on the surface of the vascular epithelium, potentially leading to the recruitment or migration of endothelial cells [28, 29]. It was also reported that when shock waves were used to treat spinal cord injury rats, it reduced the neural tissue damage, enhanced the effectiveness of neuroprotection, and improved motor function without any detrimental effect [30].

In both cases A and B treated by transcranial TMI, no damage or impairment of the surrounding brain tissue could be observed. On the contrary, wishful effects of neuromodulation and neurostimulation may be achieved.

Neuromodulation and neurostimulation

Neuromodulation and neurostimulation are used to treat neurological disorders. Acoustic energy can be applied to local regions of the brain, including deep brain structures.

Focused ultrasound may induce the activation or inhibition of nerves through parameter adjustments. In the rat model, transcranial ultrasonic stimulation is pressure- and anesthesia-dependent in the rat model. Numerical simulations have shown that the acoustic pattern can be complex inside the rat head and that special care must be taken for small animal studies relating acoustic parameters to neurostimulation effects, especially at a low frequency [31-35]. Very recently it was shown that transcranial focused ultrasound stimulation enhances semantic memory by modulating brain morphology, neurochemistry and neural dynamics [36].

Focused shock wave therapy has been used to increase alertness and awareness of patients with chronic disorders of consciousness [37]. There have been few studies of neurostimulation using shock waves with pulse durations of several nanoseconds. In an experimental study in three rats, neurostimulation was initiated by shock waves generated from a focused carbon nanotube transducer. The number of peaks of electroencephalographic signals was measured significantly higher after shock wave stimulation than before stimulation in all three rats. This study provides a basis for the applications of shock waves to brain stimulation for precise targeting [38].

In our paradigmatic patient A, the fulminant development of diffuse cerebral metastases could not be controlled with conventional surgical, radiotherapeutic, and pharmacological methods and led to the patient being in a severe palliative situation. In this situation, transcranial electrohydraulic TMI treatment resulted in unexpected clinical stabilization within eight weeks, a measurable cessation of further metastasis as demonstrated by imaging, and slow, ongoing regeneration of all neurological capacities. This clinical regeneration may be an effect of TMI treatment exerting positive effects of neuromodulation and neurostimulation by the regular application of unfocused shock waves to the entire cerebrum at a low energy flux density of a maximum of 0.04 mJ/mm^2. The clinical effects were observed within short time after TMI treatment and have been sustained. We suppose that the combination of focused tumor-destructive piezoelectric and electrohydraulic

treatments with separate, subsequent unfocused electrohydraulic treatment contributed significantly to the repeated success in the present case.

Other molecular mechanisms

The currently proposed cellular and molecular mechanisms of the brain tissue's response to extracorporeal shock wave treatment further comprise the mediation of the expression of pro-and anti-inflammatory cytokines, closing of the voltage-gated sodium channels to nociceptive input, activation of serotonin in the cerebral cortex, and reduction of the production of substance P and calcitonin gene-related peptide (CGRP) in the dorsal root ganglion [details are reviewed in 39].

Conclusions

First, by applying transcranial TMI treatment we did not observe identifiable signs that the intact surrounding brain tissue would be impaired, and TMI treatment may, therefore, provide another option for the therapy of primary or secondary malignant brain tumors. On the contrary, there are indications that shock waves could even contribute to wishful regeneration mechanisms within the brain tissue.

Second, transcranial TMI can temporarily open the blood-brain-barrier so that intracerebral immunological responses are enabled. Although the presented results of transcranial TMI treatment for brain metastases appear promising, and no clinical deterioration by TMI treatment has occurred, further cases of transcranial TMI treatments as in the planned randomized clinical trials will reveal the true efficacy of this therapeutic measure.

Acknowledgements

Author Contributions

A.E. Theuer and G.F. Walter, with the scientific support of F. Lang, proved the fundamental biological feasibility of the treatment of cancer applying TMI.

S. Exner, I. Thomas, the sadly deceased G. Strassmann, T.K. Eigentler, J.D. Mullins and J. Warlick helped to transform the concept into actual clinical practice.

G.F. Walter wrote the manuscript.

Disclosure Statement

The authors declare that they have no competing interests.

References

1 Theuer AE, Walter GF: Device and arrangement for destroying tumor cells and tumor tissue. German Patent WO002009156156A1 / 2009.

2 Theuer AE, Walter GF: Apparatus for the destruction of tumor cells or pathogens in the blood stream. German Patent WO002010406A1 / 2010.

3 Theuer AE, Walter GF: Medical device for treating tumor tissue. German Patent WO002010049176A1 / 2010

4 Theuer AE, Theuer I: Device for treating malignant diseases with the help of tumor-destructive mechanical pulses (TMI). U.S. Patent US20200038694 / 2023.

5 Theuer AE, Thomas I, Lang F, Borkmann M, Mullins JD, Eigentler TK, Walter GF. Tumor Destructive Mechanical Impulse (TMI) Treatment of Solid Tumors. Part I: Animal Experiments, Clinical Application and Immunological Abscopal Effect. Cell Physiol Biochem. 202;59(6):800-810.

6 Theuer AE, Schierbaum N, Niessner H, Sinnberg TW, Schäffer TE, Lange F, Mullins JD, Eigentler TK, Walter GF. Tumor Destructive Mechanical Impulse (TMI) Treatment of Solid Tumors. Part II: Biomechanics, Computational Simulation, Technical Generator and Applicator Design, and Physiological Effect. Cell Physiol Biochem. 2026;60(1):30-43.
7 Roberts JW, Powlovich L, Sheybani N, LeBlang S. Focused ultrasound for the treatment of glioblastoma. J Neurooncol. 2022;157:237-247.
8 Duclos S, Golin A, Fox A, Chaudhary N, Camelo-Piragua S, Pandey A, Xu Z. Transcranial histotripsy parameter study in primary and metastatic murine brain tumor models. Int J Hyperthermia. 2023;40:2237218.
9 Khagi S, Kotecha R, Gatson NTN, Jeyapalan S, Abdullah HI, Avgeropoulos NG, Batzianouli ET, Giladi M, Lustgarten L, Goldlust SA: Recent advances in Tumor Treating Fields (TTFields) therapy for glioblastoma. Oncologist. 2025;30:oyae227.
10 PiezoWave^2 https://www.elvation.de/en/piezo-systems/extracorporeal-shockwave-therapy-eswt/piezowave2t/
11 OrthoGold100®. https://softwavetrt.com/wp-content/uploads/2021/08/Instructions-for-Use.pdf
12 Duffy MJ. Cellular oncogenes and suppressor genes as prognostic markers in cancer. Clin Biochem. 1993;26(6):439-447.
13 Walter GF. Gliomas and the p53 gene and protein. Crit Rev Neurosurg. 1994;4:393-400.
14 Carpentier A, Canney M, Vignot A, Reina V, Beccaria K, Horodyckid C, Karachi C, Leclercq D, Lafon C, Chapelon JY, Capelle L, Cornu P, Sanson M, Hoang-Xuan K, Delattre JY, Idbaih A. Clinical trial of blood-brain barrier disruption by pulsed ultrasound. Sci Transl Med. 2016;8:343re2.
15 Idbaih A, Canney M, Belin L, Desseaux C, Vignot A, Bouchoux G, Asquier N, Law-Ye B, Leclercq D, Bissery A, De Rycke Y, Trosch C, Capelle L, Sanson M, Hoang-Xuan K, Dehais C, Houillier C, Laigle-Donadey F, Mathon B, André A, Lafon C, Chapelon JY, Delattre JY, Carpentier A. Safety and feasibility of repeated and transient blood-brain barrier disruption by pulsed ultrasound in patients with recurrent glioblastoma. Clin Cancer Res. 2019;25(13):3793-3801.
16 Carpentier A, Stupp R, Sonabend AM, Dufour H, Chinot O, Mathon B, Ducray F, Guyotat J, Baize N, Menei P, de Groot J, Weinberg JS, Liu BP, Guemas E, Desseaux C, Schmitt C, Bouchoux G, Canney M, Idbaih A. Repeated blood-brain barrier opening with a nine-emitter implantable ultrasound device in combination with carboplatin in recurrent glioblastoma: a phase I/II clinical trial. Nat Commun. 2024;15(1):1650.
17 Monden Y, Tsukamoto A, Ushida T, Kobayashi E, Nakagawa K, Sakuma I. An *in vitro* model of temporal enhancement of epithelium barrier permeability by low-energy shock waves without contrast agents. Med Biol Eng Comput. 2020;58(9):1987-1993.
18 Zhou M, Zhou W, Yang H, Cao L, Li M, Yin P, Zhou Y. Molecular modeling of shockwave-mediated blood-brain barrier opening for targeted drug delivery. ACS Appl Mater Interfaces. 2024;16(16):20212-20220.
19 Kung Y, Lan C, Hsiao MY, Sun MK, Hsu YH, Huang AP, Liao WH, Liu HL, Inserra C, Chen WS. Focused shockwave induced blood-brain barrier opening and transfection. Sci Rep. 2018 Feb 2;8(1):2218.
20 Woodworth GF, Anastasiadis P, Ozair A, Chabros J, Bettegowda C, Chen C, Gerstl JVE, Douville C, Mekary RA, Smith TR, Meng Y, Hawkins C, Pople CB, Abrahao A, Llinas M, Heyn C, Bunevicius A, Rezai AR, Ball AJS, Henry K, Sahgal A, Torio E, Ren H, Ahmad H, Arora H, Eisenberg H, Perry J, Carpenter JS, Hynynen K, Pham LC, Anketell MB, Lim-Fat MJ, Xu Z, Cifarelli CP, Sheehan JP, McDannold NJ, Gandhi D, Golby AJ, Lipsman N. Microbubble-enhanced transcranial focused ultrasound with temozolomide for patients with high-grade glioma (BT008NA): a multicentre, open-label, phase 1/2 trial. Lancet Oncol. 2025;26(12):1651-1664. doi: 10.1016/S1470-2045(25)00492-9.
21 Obeid MA, Alsaadi M, Aljabali AA. Recent updates in curcumin delivery. J Liposome Res. 2023;33(1):53-64.
22 Ratan C, Arian AM, Rajendran R, Jayakumar R, Masson M, Mangalathillam S. Nano-based formulations of curcumin: elucidating the potential benefits and future prospects in skin cancer. Biomed Mater. 2023;18(5).
23 Taylor PA, Ludwigsen JS, Ford CC. Investigation of blast-induced traumatic brain injury. Brain Inj. 2014;28(7):879-95.
24 Yu B, Wang H, Fan X, Li L, Li X, Zhang Y, Ma J, Ma N, Wang Q, Lu Q, Gao J. Experimental analysis of blast shock wave-induced injuries in rats: Neurobehavioral and tissue damage assessments. Exp Neurol. 2025;394:115427.

25 Adhikarla SV, Jha NK, Goswami VK, Sharma A, Bhardwaj A, Dey A, Villa C, Kumar Y, Jha SK. TLR-Mediated Signal Transduction and Neurodegenerative Disorders. Brain Sci. 2021;11(11):1373. doi: 10.3390/brainsci11111373.
26 Gollmann-Tepeköylü C, Nägele F, Graber M, Pölzl L, Lobenwein D, Hirsch J, An A, Irschick R, Röhrs B, Kremser C, Hackl H, Huber R, Venezia S, Hercher D, Fritsch H, Bonaros N, Stefanova N, Tancevski I, Meyer D, Grimm M, Holfeld J. Shock waves promote spinal cord repair via TLR3. JCI Insight. 2020;5(15):e134552. doi: 10.1172/jci.insight.134552.
27 Nakagawa A, Kusaka Y, Hirano T, Saito T, Shirane R, Takayama K, Yoshimoto T. Application of shock waves as a treatment modality in the vicinity of the brain and skull. J Neurosurg. 2003;99(1):156-162. doi: 10.3171/jns.2003.99.1.0156.
28 Yamaya S, Ozawa H, Kanno H, Kishimoto KN, Sekiguchi A, Tateda S, Yahata K, Ito K, Shimokawa H, Itoi E. Low-energy extracorporeal shock wave therapy promotes vascular endothelial growth factor expression and improves locomotor recovery after spinal cord injury. J Neurosurg. 2014;121(6):1514-1525. 10.3171/2014.8.JNS132562.
29 Yahata K, Kanno H, Ozawa H, Yamaya S, Tateda S, Ito K, Shimokawa H, Itoi E. Low-energy extracorporeal shock wave therapy for promotion of vascular endothelial growth factor expression and angiogenesis and improvement of locomotor and sensory functions after spinal cord injury. J Neurosurg Spine. 2016;25(6):745-755. doi: 10.3171/2016.4.SPINE15923.
30 Matsuda M, Kanno H, Sugaya T, Yamaya S, Yahata K, Handa K, Shindo T, Shimokawa H, Ozawa H, Itoi E. Low-energy extracorporeal shock wave therapy promotes BDNF expression and improves functional recovery after spinal cord injury in rats. Exp Neurol. 2020;328:113251. doi: 10.1016/j.expneurol.2020.113251.
31 Younan Y, Deffieux T, Larrat B, Fink M, Tanter M, Aubry JF. Influence of the pressure field distribution in transcranial ultrasonic neurostimulation. Med Phys. 2013;40(8):082902.
32 Park TY, Pahk KJ, Kim H. Method to optimize the placement of a single-element transducer for transcranial focused ultrasound. Comput Methods Programs Biomed. 2019;179:104982.
33 Peng D, Tong W, Collins DJ, Ibbotson MR, Prawer S, Stamp M. Mechanisms and applications of neuromodulation using surface acoustic waves-A mini-review. Front Neurosci. 2021;15:629056.
34 Nguyen DT, Berisha DE, Konofagou EE, Dmochowski JP. Neuronal responses to focused ultrasound are gated by pre-stimulation brain rhythms. Brain Stimul. 2022;15(1):233-243.
35 Chen M, Peng C, Wu H, Huang CC, Kim T, Traylor Z, Muller M, Chhatbar PY, Nam CS, Feng W, Jiang X. Numerical and experimental evaluation of low-intensity transcranial focused ultrasound wave propagation using human skulls for brain neuromodulation. Med Phys. 2023;50(1):38-49.
36 Jung J, Atkinson-Clement C, Kaiser M, Lambon Ralph MA. Transcranial focused ultrasound stimulation enhances semantic memory by modulating brain morphology, neurochemistry and neural dynamics. Nat Commun. 2026 Feb 16. doi: 10.1038/s41467-026-69579-7. Epub ahead of print. PMID: 41698912.
37 Werner C, Byhahn M, Hesse S. Non-invasive brain stimulation to promote alertness and awareness in chronic patients with disorders of consciousness: Low-level, near-infrared laser stimulation vs. focused shock wave therapy. Restor Neurol Neurosci. 2016;34(4):561-569. doi: 10.3233/RNN-150624.
38 Lee J, Larocco JW, Paeng DG. Electroencephalographic response of brain stimulation by shock waves from laser generated carbon nanotube transducer. IEEE Trans Neural Syst Rehabil Eng. 2023;31:398-405.
39 Guo J, Hai H, Ma Y. Application of extracorporeal shock wave therapy in nervous system diseases: A review. Front Neurol. 2022;13:963849.